

Elastic analysis of pressurized thick truncated conical shells made of functionally graded materials

M. Ghannad^{1a}, M. Zamani Nejad^{*2}, G.H. Rahimi^{3b} and H. Sabouri^{3a}

¹Mechanical Engineering Faculty, Shahrood University of Technology, Shahrood, Iran

²Mechanical Engineering Department, Yasouj University, Yasouj P.O. Box: 75918-74831, Iran

³Mechanical Engineering Department, Tarbiat Modares University, Tehran, Iran

(Received December 21, 2011, Revised April 26, 2012, Accepted May 31, 2012)

Abstract. Based on the first-order shear deformation theory (FSDT), and the virtual work principle, an elastic analysis for axisymmetric clamped-clamped Pressurized thick truncated conical shells made of functionally graded materials have been performed. The governing equations are a system of nonhomogeneous ordinary differential equations with variable coefficients. Using the matched asymptotic method (MAM) of the perturbation theory, these equations could be converted into a system of algebraic equations with variable coefficients and two systems of differential equations with constant coefficients. For different FGM conical angles, displacements and stresses along the radius and length have been calculated and plotted.

Keywords: truncated conical shells; thick-walled; functionally graded material (FGM); analytical solution; perturbation technique

1. Introduction

As truncated conical shells have widely been applied in many fields such as space flight, rocket, aviation, and submarine technology, and the like, their stress analysis is inevitable in engineering. The literature that addresses the stresses of thick conical shells is quite limited. Most of the existing literature deals with the stress or vibration analysis of thin conical shells and it is based upon a thin shell or membrane shell theory, whereas very little attention has been paid to the analytical solution of thick conical shells, which is due to the limitations of the classic theories of thick wall shells.

Functionally graded materials (FGMs) are a new type of composite materials with continuously varied microstructure, which lead to the continuous variation of physical and mechanical properties through the thickness. The graded changes in the composition of FGMs can reduce or even eliminate the specific interfaces between constituent materials, and avoid the initiation of cracks. FGMs are applicable to many engineering fields. Such as aerospace, nuclear energy, chemical plant, electronics, biomaterials and so on.

*Corresponding author, Assistant Professor, E-mail: m.zamani.n@gmail.com

^aAssistant Professor

^bProfessor

Perturbation technique can be used for solving the nonhomogeneous ordinary and partial differential equations (ODE and PDE) with variable coefficients. These equations normally do not have exact solutions. In fact, this technique converts the equation or set equations into solvable equations. This method is applicable in different branches of sciences and engineering. In solid mechanics, for the purpose of analysis in different structures including beams (Ozturk and Coskun 2011, Pan *et al.* 2011) and shells, this method utilized.

Considering the cross shear effect, Naghdi and Cooper (1956), formulated the theory of shear deformation. Using the FSDT, Mirsky and Hermann (1958), obtained the solution of thick cylindrical shells of homogenous and isotropic materials. Assuming the cone is to be long and the angle of the lateral side with a horizontal plane is great, Hausenbauer and Lee (1966) obtained the radial, tangential and axial wall stresses in a thick-walled cone under internal and/or external pressure. McDonald and Chang (1973) applied the asymptotic method to Donnell's equations for analysis of conical shells. Using the shear deformation theory and Frobenius series, Takashaki *et al.* (1986), obtained the solution of free vibration of conical shells with variable thickness. Sundarasivarao and Ganesan (1991) analyzed a conical shell under pressure using the FEM. Chaudhry *et al.* (1996) modeled the left ventricle as a thick truncated conical shell, which was assumed isotropic, elastic with large deformation while three-dimensional equations of elasticity have been simplified for this special shape. Eipakchi *et al.* (2003), obtained the solution of the homogenous and isotropic thick-walled cylindrical shells with variable thickness, using the FSDT and the perturbation theory. Eipakchi *et al.* (2008) used the mathematical approach based on the perturbation theory, for elastic analysis a thick conical shell with varying thickness under nonuniform internal pressure. Based on the FSDT and the virtual work principle, an elastic solution for thick truncated conical shells (Ghannad *et al.* 2009), an elastic solution for clamped-clamped thick cylindrical shells (Ghannad and Nejad 2010) and an elastic solution for thick cylindrical shells with variable thickness (Ghannad *et al.* 2012) are obtained. A complete and consistent three-dimensional set of field equations has been developed by tensor analysis to characterize the behavior of FGM thick shells of revolution with arbitrary curvature and variable thickness along the meridional direction (Nejad *et al.* 2009). The finite element method (FEM) based on the Rayleigh-Ritz energy formulation applied to obtain the elastic behavior of the functionally graded thick truncated cone (Asemi *et al.* 2010). Using third-order shear deformation theory, an analytical solution presented for stresses and displacements in a thick conical shell with varying thickness under nonuniform internal pressure (Eipakchi 2010). Assuming the material composition varying continuously along its thickness according to the power law distribution, dynamic analysis of a thick truncated cone made of a combined ceramic-metal material with finite length under axisymmetric internal impact loading is studied by Asemi *et al.* (2010). In other study, using the finite element method based on Rayleigh-Ritz energy formulation, the elastic behavior of the functionally graded thick truncated cone with finite length, and is subjected to axisymmetric hydrostatic internal pressure, are investigated (Asemi *et al.* 2011).

In the present work, an attempt has been made to find the analytical solution of the functionally graded thick truncated conical shells, by using the FSDT. The governing equations in the axisymmetric case and elastostatic state, which are a system of ordinary differential equations with variable coefficients, have been solved analytically, using the MAM of the perturbation theory.

2. Analysis

In the classical theory of shells, the assumption is that the sections that are straight and perpendicular to the mid-plane remain in the same position even after deformation. In the FSDT, the sections that are straight and perpendicular to the mid-plane remain straight but not necessarily perpendicular after deformation. In this case, shear strain and shear stress are taken into consideration.

In Fig. 1, the location of a typical point m , (r), within the thick truncated conical shell element may be determined by R and z , as

$$\begin{cases} r(x, z) = R(x) + z \\ \left| \frac{z}{r} \right| < 1 \end{cases} \quad (1)$$

where R represents the distance of middle surface from the x -axes, and z is the distance of typical point from the middle surface.

In Eq. (1), x and z must be within the following ranges

$$\begin{cases} 0 \leq \frac{x}{L} \leq 1 \\ -\frac{1}{2} \leq \frac{z}{h} \leq \frac{1}{2} \end{cases} \quad (2)$$

where h and L are the thickness and the length of the cone.

The general axisymmetric displacement field (U_x, U_z), in the first-order Mirsky-Hermann's theory could be expressed, as follows

$$U_x(x, z) = u(x) + \phi(x)z, \quad U_z(x, z) = w(x) + \psi(x)z \quad (3)$$

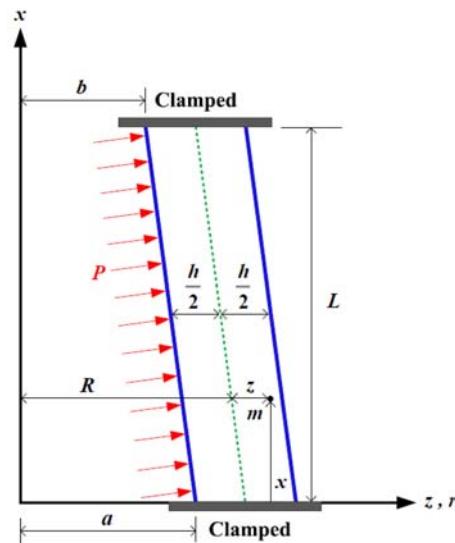


Fig. 1 Cross section of a thick-walled truncated conical shell under internal pressure

where $u(x)$ and $w(x)$ are the displacement components of the middle surface. Also, $\phi(x)$ and $\psi(x)$ are the functions used to determine the displacement field.

The strain-displacement relations in the cylindrical coordinates system are

$$\begin{cases} \varepsilon_x = \frac{\partial U_x}{\partial x} = \frac{du}{dx} + \frac{d\phi}{dx} z \\ \varepsilon_\theta = \frac{U_z}{r} = \frac{w}{R+z} + \frac{\psi}{R+z} z \\ \varepsilon_z = \frac{\partial U_z}{\partial z} = \psi \\ \gamma_{xz} = \frac{\partial U_x}{\partial z} + \frac{\partial U_z}{\partial x} = \phi + \frac{dw}{dx} + \frac{d\psi}{dx} z \end{cases} \quad (4)$$

In addition, the stresses on the basis of constitutive equations for homogenous and isotropic materials are as follows

$$\begin{cases} \sigma_x = \lambda E(x, z)[(1-\nu)\varepsilon_x + \nu(\varepsilon_\theta + \varepsilon_z)] \\ \sigma_\theta = \lambda E(x, z)[(1-\nu)\varepsilon_\theta + \nu(\varepsilon_z + \varepsilon_x)] \\ \sigma_z = \lambda E(x, z)[(1-\nu)\varepsilon_z + \nu(\varepsilon_x + \varepsilon_\theta)] \\ \tau_{xz} = \lambda E(x, z)(1-2\nu)\frac{\gamma_{xz}}{2} \end{cases} \quad (5a)$$

and

$$\lambda = \frac{1}{(1+\nu)(1-2\nu)} \quad (5b)$$

where σ_i and ε_i are the stresses and strains in the axial (x), circumferential (θ), and radial (z) directions. ν and $E(x, z)$ are Poisson's ratio and modulus of elasticity, respectively.

The normal forces (N_x, N_θ, N_z), shear force (Q_x), bending moments (M_x, M_θ), and the torsional moment (M_{xz}) in terms of stress resultants are

$$\begin{Bmatrix} N_x \\ N_\theta \\ N_z \end{Bmatrix} = \int_{-h/2}^{h/2} \begin{Bmatrix} \sigma_x \left(1 + \frac{z}{R}\right) \\ \sigma_\theta \\ \sigma_z \left(1 + \frac{z}{R}\right) \end{Bmatrix} dz \quad (6)$$

$$\begin{Bmatrix} M_x \\ M_\theta \\ M_z \end{Bmatrix} = \int_{-h/2}^{h/2} \begin{Bmatrix} \sigma_x \left(1 + \frac{z}{R}\right) \\ \sigma_\theta \\ \sigma_z \left(1 + \frac{z}{R}\right) \end{Bmatrix} z dz \quad (7)$$

$$Q_x = \int_{-h/2}^{h/2} \tau_{xz} \left(1 + \frac{z}{R}\right) dz \quad (8)$$

$$M_{xz} = \int_{-h/2}^{h/2} \tau_{xz} \left(1 + \frac{z}{R}\right) z dz \quad (9)$$

On the basis of the principle of virtual work, the variations of strain energy are equal to the variations of the external work as follows

$$\delta U = \delta W \quad (10)$$

where U is the total strain energy of the elastic body and W is the total external work due to internal pressure. The strain energy is

$$\begin{cases} U = \iiint_V U^* dV, & dV = r dr d\theta dx = (R+z) dz d\theta dx \\ U^* = \frac{1}{2} (\sigma_x \varepsilon_x + \sigma_\theta \varepsilon_\theta + \sigma_z \varepsilon_z + \tau_{xz} \gamma_{xz}) \end{cases} \quad (11)$$

and the external work is

$$W = \iint_S (\vec{f} \cdot \vec{u}) dS, \quad dS = r_i d\theta dx = \left(R - \frac{h}{2}\right) d\theta dx \quad (12)$$

where

$$\begin{cases} \vec{f} \cdot \vec{u} = P_x U_x + P_z U_z \\ P_x = \frac{(a-b)P}{\sqrt{(a-b)^2 + L^2}}, \quad P_z = \frac{LP}{\sqrt{(a-b)^2 + L^2}} \end{cases} \quad (13)$$

Here P_x and P_z are components of internal pressure P along axial and radial directions, respectively.

The variation of the strain energy is

$$\delta U = \int_0^{2\pi} \int_0^L \int_{-h/2}^{h/2} R(x) \delta U^* \left(1 + \frac{z}{R}\right) dz dx d\theta \quad (14)$$

The resulting of Eq. (14) is

$$\frac{\delta U}{2\pi} = \int_0^L R(x) \int_{-h/2}^{h/2} (\sigma_x \delta \varepsilon_x + \sigma_\theta \delta \varepsilon_\theta + \sigma_z \delta \varepsilon_z + \tau_{xz} \delta \gamma_{xz}) \left(1 + \frac{z}{R}\right) dz dx \quad (15)$$

and the variation of the external work is

$$\delta W = \int_0^{2\pi} \int_0^L (P_x \delta U_x + P_z \delta U_z) \left(R - \frac{h}{2}\right) dx d\theta \quad (16)$$

The resulting Eq. (16) will be

$$\frac{\delta W}{2\pi} = \int_0^L (P_x \delta U_x + P_z \delta U_z) \left(R - \frac{h}{2} \right) dx \quad (17)$$

Substituting Eqs. (4) and (5) into Eqs. (15) and (17), and by considering the virtual work principle (Eq. 10), we will have

$$\begin{cases} \frac{d}{dx}(RN_x) = -P_x \left(R - \frac{h}{2} \right) \\ \frac{d}{dx}(RM_x) - RQ_x = P_x \frac{h}{2} \left(R - \frac{h}{2} \right) \\ \frac{d}{dx}(RQ_x) - N_\theta = -P_z \left(R - \frac{h}{2} \right) \\ \frac{d}{dx}(RM_{xz}) - M_\theta - RN_z = P_z \frac{h}{2} \left(R - \frac{h}{2} \right) \end{cases} \quad (18)$$

And the boundary conditions are

$$[R(N_x \delta u + M_x \delta \phi + Q_x \delta w + M_{xz} \delta \psi)]_0^L = 0 \quad (19)$$

Eq. (19) states the boundary conditions which must exist at the two ends of the cone.

3. Modeling of FGM thick-walled truncated cone

Nonhomogenous and isotropic FG materials have the same material properties in directions. However, their properties are different in terms of points. In such materials, changes of properties are generally considered in radial or longitudinal directions.

The modulus of elasticity in FG thick truncated conical shell in terms of two radial (z) and longitudinal (x) variables is assumed as follows

$$E(x, z) = \frac{E_i}{b^n} \left[a - (a-b) \frac{x}{L} + \frac{h}{2} + z \right]^n \quad (20)$$

In this equation, E_i refers to the modulus of elasticity of that point of inner surface in which $x = L$ and n is the inhomogeneity constants determined empirically.

Based on Eq. (20), the modulus of elasticity in all the points which have equal distance to symmetrical axis is the same. This means manufacturing FG conical shells by fitting numerous homogenous cylinders of variable length.

4. Analytical solution for $n = +1$

The modulus of elasticity is:

$$E(x, z) = \frac{E_i}{2bL} [L(2a + 2z + h) - 2(a - b)x] \quad (21)$$

By substituting Eqs. (4) and (21) into Eqs. (5), and then using Eqs. (6) to (9), forces and moments are obtained as follows

$$N_x = \lambda \frac{E_i}{b} \left[(1-\nu) \left(Rh + \frac{h^3}{12R} \right) \frac{du}{dx} + (1-\nu) \left(\frac{h^3}{6} \right) \frac{d\phi}{dx} + \nu hw + \nu \left(Rh + \frac{h^3}{6R} \right) \psi \right] \quad (22a)$$

$$N_\theta = \lambda \frac{E_i}{b} \left[\nu Rh \frac{du}{dx} + \nu \left(\frac{h^3}{12} \right) \frac{d\phi}{dx} + (1-\nu)hw + \nu Rh\psi \right] \quad (22b)$$

$$N_z = \lambda \frac{E_i}{b} \left[\nu \left(Rh + \frac{h^3}{12R} \right) \frac{du}{dx} + \nu \left(\frac{h^3}{6} \right) \frac{d\phi}{dx} + \nu hw + \left((1-\nu)Rh + \frac{h^3}{12R} \right) \psi \right] \quad (22c)$$

$$M_x = \lambda \frac{E_i}{b} \left[(1-\nu) \left(\frac{h^3}{6} \right) \frac{du}{dx} + (1-\nu) \left(\frac{Rh^3}{12} + \frac{h^5}{80R} \right) \frac{d\phi}{dx} + \nu \frac{h^3}{12R} w + \nu \frac{h^3}{4} \psi \right] \quad (23a)$$

$$M_\theta = \lambda \frac{E_i}{b} \left[\nu \left(\frac{h^3}{12} \right) \frac{du}{dx} + \nu \frac{Rh^3}{12} \frac{d\phi}{dx} + \frac{h^3}{12} \psi \right] \quad (23b)$$

$$M_z = \lambda \frac{E_i}{b} \left[\nu \left(\frac{h^3}{6} \right) \frac{du}{dx} + \nu \left(\frac{Rh^3}{12} + \frac{h^5}{80R} \right) \frac{d\phi}{dx} + \nu \frac{h^3}{12R} w + (2-\nu) \frac{h^3}{12} \psi \right] \quad (23c)$$

$$Q_x = \frac{K}{2} (1-2\nu) \lambda \frac{E_i}{b} \left[\left(Rh + \frac{h^3}{12R} \right) \left(\phi + \frac{dw}{dx} \right) + \frac{h^3}{6} \frac{d\psi}{dx} \right] \quad (24)$$

$$M_{xz} = \frac{K}{2} (1-2\nu) \lambda \frac{E_i}{b} \left[\frac{h^3}{6} \left(\phi + \frac{dw}{dx} \right) + \left(\frac{Rh^3}{12} + \frac{h^5}{80R} \right) \frac{d\psi}{dx} \right] \quad (25)$$

where K is the shear correction factor that is embedded in the shear stress term. It is assumed that in the static state, for conical shells $K = 5/6$ (Vlachoutsis 1992).

In order to solve the set of differential Eq. (18), forces and moments need to be expressed in terms of the components of displacement field. Substituting Eqs. (22) to (25) into Eqs. (18), set of differential Eq. (18) may be rewritten as follows

$$\begin{cases} \frac{d}{dx} \left([B_1] \frac{d}{dx} \{y'\} \right) + \frac{d}{dx} ([B_2] \{y'\}) + [B_3] \frac{d}{dx} \{y'\} + [B_4] \{y'\} = \{F'\} \\ \{y'\} = \{u(x) \quad \phi(x) \quad w(x) \quad \psi(x)\}^T \end{cases} \quad (26)$$

where the coefficients matrices $[B_i]_{4 \times 4}$, and the force vector $\{F'\}$ are as follows

$$[B_1] = \begin{bmatrix} \frac{(1-\nu)h}{12L^2}(3(\gamma(x))^2 + h^2L^2) & \frac{(1-\nu)h^3}{12L}\gamma(x) & 0 & 0 \\ \frac{(1-\nu)h^3}{12L}\gamma(x) & \frac{(1-\nu)h^3}{240L^2}(5(\gamma(x))^2 + 3h^2L^2) & 0 & 0 \\ 0 & 0 & \frac{\Lambda h}{12L^2}(3(\gamma(x))^2 + h^2L^2) & \frac{\Lambda h^3}{12L}\gamma(x) \\ 0 & 0 & \frac{\Lambda h^3}{12L}\gamma(x) & \frac{\Lambda h^3}{240L^2}(5(\gamma(x))^2 + 3h^2L^2) \end{bmatrix} \quad (27a)$$

$$[B_2] = \begin{bmatrix} 0 & 0 & \frac{\nu h}{2L}\gamma(x) & \frac{\nu h}{24L^2}(6(\gamma(x))^2 + 4h^2L^2) \\ 0 & 0 & \frac{\nu h^3}{12} & \frac{\nu h^3}{8L}\gamma(x) \\ 0 & \frac{\Lambda h}{12L^2}(3(\gamma(x))^2 + h^2L^2) & 0 & 0 \\ 0 & \frac{\Lambda h^3}{12L}\gamma(x) & 0 & 0 \end{bmatrix} \quad (27b)$$

$$[B_3] = \begin{bmatrix} 0 & 0 & 0 & 0 \\ 0 & 0 & -\frac{\Lambda h}{12L^2}(3(\gamma(x))^2 + h^2L^2) & -\frac{\Lambda h^3}{12L}\gamma(x) \\ -\frac{\nu h}{2L}\gamma(x) & -\frac{\nu h^3}{12} & 0 & 0 \\ -\frac{\nu h}{24L^2}(6(\gamma(x))^2 + 4h^2L^2) & -\frac{\nu h^3}{8L}\gamma(x) & 0 & 0 \end{bmatrix} \quad (27c)$$

$$[B_4] = \begin{bmatrix} 0 & 0 & 0 & 0 \\ 0 & -\frac{\Lambda h}{12L^2}(3(\gamma(x))^2 + h^2L^2) & 0 & 0 \\ 0 & 0 & -(1-\nu)h & -\frac{\nu h}{2L}\gamma(x) \\ 0 & 0 & -\frac{\nu h}{2L}\gamma(x) & -\frac{(1-\nu)h}{4L^2}(\gamma(x))^2 - \frac{h^3}{6} \end{bmatrix} \quad (27d)$$

$$\{F'\} = \frac{b}{\lambda E_i} \left(a + \frac{\nabla_2}{2L} x \right) \begin{Bmatrix} -P_x \\ \frac{h}{2} P_x \\ -P_z \\ \frac{h}{2} P_z \end{Bmatrix} \quad (27e)$$

and

$$\begin{cases} \gamma(x) = \forall_1 + \forall_2 x \\ \forall_1 = L(2a + h) \\ \forall_2 = 2(b - a) \\ \Lambda = K \frac{(1 - 2\nu)}{2} \end{cases} \quad (28)$$

$[B_4]$ do not have inverse and its reverse is needed in the next calculations. In order to make $[B_4]^{-1}$, the first equation in the set of Eqs. (18) is integrated.

$$RN_x = -\int P_x \left(R - \frac{h}{2} \right) dx + C_0 \quad (29)$$

Taking du/dx as v ,

$$u = -\int v dx + C_7 \quad (30)$$

Thus, set of differential Eq. (26) could be derived as follows

$$\begin{cases} \frac{d}{dx} \left([A_1] \frac{d}{dx} \{y\} \right) + \frac{d}{dx} ([A_2] \{y\}) + [A_3] \frac{d}{dx} \{y\} + [A_4] \{y\} = \{F\} \\ \{y\} = \{v(x) \quad \phi(x) \quad w(x) \quad \psi(x)\}^T \end{cases} \quad (31)$$

where the coefficients matrices $[A_i]_{4 \times 4}$, and the force vector $\{F\}$ are as follows

$$[A_1] = \begin{bmatrix} 0 & 0 & 0 & 0 \\ 0 & \frac{(1-\nu)h^3}{240L^2} (5(\gamma(x))^2 + 3h^2L^2) & 0 & 0 \\ 0 & 0 & \frac{\Lambda h}{12L^2} (3(\gamma(x))^2 + h^2L^2) & \frac{\Lambda h^3}{12L} \gamma(x) \\ 0 & 0 & \frac{\Lambda h^3}{12L} \gamma(x) & \frac{\Lambda h^3}{240L^2} (5(\gamma(x))^2 + 3h^2L^2) \end{bmatrix} \quad (32a)$$

$$[A_2] = \begin{bmatrix} 0 & 0 & 0 & 0 \\ \frac{(1-\nu)h^3}{12L} \gamma(x) & 0 & \frac{\nu h^3}{12} & \frac{\nu h^3}{8L} \gamma(x) \\ 0 & \frac{\Lambda h}{12L^2} (3(\gamma(x))^2 + h^2L^2) & 0 & 0 \\ 0 & \frac{\Lambda h^3}{12L} \gamma(x) & 0 & 0 \end{bmatrix} \quad (32b)$$

$$[A_3] = \begin{bmatrix} 0 & \frac{(1-\nu)h^3}{12L}Y(x) & 0 & 0 \\ 0 & 0 & -\frac{\Lambda h}{12L^2}(3(Y(x))^2 + h^2L^2) & -\frac{\Lambda h^3}{12L}Y(x) \\ 0 & -\frac{\nu h^3}{12} & 0 & 0 \\ 0 & -\frac{\nu h^3}{8L}Y(x) & 0 & 0 \end{bmatrix} \quad (32c)$$

$$[A_4] = \begin{bmatrix} \frac{(1-\nu)h}{12L^2}(3(Y(x))^2 + h^2L^2) & 0 & \frac{\nu h}{2L}Y(x) & \frac{\nu h}{24L^2}(6(Y(x))^2 + 4h^2L^2) \\ 0 & -\frac{\Lambda h}{12L^2}(3(Y(x))^2 + h^2L^2) & 0 & 0 \\ -\frac{\nu h}{2L}Y(x) & 0 & -(1-\nu)h & -\frac{\nu h}{2L}Y(x) \\ -\frac{\nu h}{24L^2}(6(Y(x))^2 + 4h^2L^2) & 0 & -\frac{\nu h}{2L}Y(x) & -\frac{(1-\nu)h}{4L^2}(Y(x))^2 - \frac{h^3}{6} \end{bmatrix} \quad (32d)$$

$$\{F\} = \frac{b}{\lambda E_i} \left\{ \begin{array}{l} -\int P_x \left(a + \frac{\nabla_2}{2L}x \right) dx + C_0 \\ P_x \frac{h}{2} \left(a + \frac{\nabla_2}{2L}x \right) \\ -P_z \left(a + \frac{\nabla_2}{2L}x \right) \\ P_z \frac{h}{2} \left(a + \frac{\nabla_2}{2L}x \right) \end{array} \right\} \quad (32e)$$

The Eq. (31) is a set of linear non-homogenous differential equations with variable coefficients.

4.1 Perturbation technique ($n = +1$)

The set of differential Eq. (31) do not have exact solutions. Perturbation theory provides a suitable method for the solution of the set of differential equations for which there are no exact solutions. For the purpose of solving, MAM of the perturbation theory has been used, in which the convergence of solution is fast. For the solution of the set of differential equations, using the perturbation theory, first, it must be made dimensionless to obtain the perturbation parameter.

The ratio of h/L is taken as the small perturbation parameter (ε). The longer the conical shell, the smaller the perturbation parameter, leading to faster convergence. $x^* = x/L$ is taken as the

dimensionless form of x . The other parameters are made dimensionless based on the thickness (h).

Solving the equations with variable coefficients gives rise to solving a system of algebraic equations and two systems of differential equations with constant coefficients. These systems of equations have the closed forms solutions. To accomplish this, making use of the characteristic scales, the governing equations are made dimensionless as follows

$$\begin{cases} x^* = \frac{x}{L}, & z^* = \frac{z}{h} \\ h^* = \frac{h}{h}, & R^* = \frac{R}{h} \\ u^* = \frac{u}{h}, & w^* = \frac{w}{h} \end{cases} \quad (33)$$

Substituting dimensionless parameters into the set of Eqs. (31)

$$\begin{cases} \varepsilon^2 \frac{d}{dx^*} \left([A_1^*] \frac{d}{dx^*} \{y^*\} \right) + \varepsilon \left[\frac{d}{dx^*} ([A_2^*] \{y^*\}) + [A_3^*] \frac{d}{dx^*} \{y^*\} \right] + [A_4^*] \{y^*\} = \{F^*\} \\ \{y^*\} = \{v \quad \phi \quad w^* \quad \psi\}^T \end{cases} \quad (34)$$

where

$$v = \frac{du}{dx} = \varepsilon \frac{du^*}{dx^*} \quad (35)$$

The coefficients matrices $[A_i^*]_{4 \times 4}$, and the force vector $\{F^*\}$ are obtained as follows

$$[A_1^*] = \begin{bmatrix} 0 & 0 & 0 & 0 \\ 0 & \frac{(1-\nu)}{240} [5(\mathcal{Y}^*(x^*) + \nabla_2^*)^2 + 3] & 0 & 0 \\ 0 & 0 & \frac{\Lambda}{12} [3(\mathcal{Y}^*(x^*) + \nabla_2^*)^2 + 1] & \frac{\Lambda}{12} (\mathcal{Y}^*(x^*) + \nabla_2^*) \\ 0 & 0 & \frac{\Lambda}{12} (\mathcal{Y}^*(x^*) + \nabla_2^*) & \frac{\Lambda}{240} [5(\mathcal{Y}^*(x^*) + \nabla_2^*)^2 + 3] \end{bmatrix} \quad (36a)$$

$$[A_2^*] = \begin{bmatrix} 0 & 0 & 0 & 0 \\ \frac{1-\nu}{12} (\mathcal{Y}^*(x^*) + \nabla_2^*) & 0 & \frac{\nu}{12} & \frac{\nu}{8} (\mathcal{Y}^*(x^*) + \nabla_2^*) \\ 0 & \frac{\Lambda}{12} [3(\mathcal{Y}^*(x^*) + \nabla_2^*)^2 + 1] & 0 & 0 \\ 0 & \frac{\Lambda}{12} (\mathcal{Y}^*(x^*) + \nabla_2^*) & 0 & 0 \end{bmatrix} \quad (36b)$$

$$[A_3^*] = \begin{bmatrix} 0 & \frac{1-\nu}{12}(Y^*(x^*) + \nabla_2^*) & 0 & 0 \\ 0 & 0 & -\frac{\Lambda}{12}[3(Y^*(x^*) + \nabla_2^*)^2 + 1] & -\frac{\Lambda}{12}(Y^*(x^*) + \nabla_2^*) \\ 0 & -\frac{\nu}{12} & 0 & 0 \\ 0 & -\frac{\nu}{8}(Y^*(x^*) + \nabla_2^*) & 0 & 0 \end{bmatrix} \quad (36c)$$

$$[A_4^*] = \begin{bmatrix} \frac{1-\nu}{12}[3(Y^*(x^*) + \nabla_2^*)^2 + 1] & 0 & \frac{\nu}{2}(Y^*(x^*) + \nabla_2^*) & \frac{\nu}{12}[3(Y^*(x^*) + \nabla_2^*)^2 + 2] \\ 0 & -\frac{\Lambda}{12}[3(Y^*(x^*) + \nabla_2^*)^2 + 1] & 0 & 0 \\ -\frac{\nu}{2}(Y^*(x^*) + \nabla_2^*) & 0 & -1 + \nu & -\frac{\nu}{2}(Y^*(x^*) + \nabla_2^*) \\ -\frac{\nu}{12}[3(Y^*(x^*) + \nabla_2^*)^2 + 2] & 0 & -\frac{\nu}{2}(Y^*(x^*) + \nabla_2^*) & -\frac{1-\nu}{4}(Y^*(x^*) + \nabla_2^*)^2 - \frac{1}{6} \end{bmatrix} \quad (36d)$$

$$[F^*] = \frac{1}{\lambda E_i h} \left\{ \begin{array}{l} -\frac{P_x}{\varepsilon} \int \left(a + \frac{1}{2}(h-1 + \nabla_1^* x^*) \right) dx^* + C_0^* \\ \frac{P_x}{2} \left(a + \frac{1}{2}(h-1 + \nabla_1^* x^*) \right) \\ -P_z \left(a + \frac{1}{2}(h-1 + \nabla_1^* x^*) \right) \\ \frac{P_z}{2} \left(a + \frac{1}{2}(h-1 + \nabla_1^* x^*) \right) \end{array} \right\} \quad (36e)$$

where the parameters are as follows

$$\begin{cases} Y^*(x^*) = \nabla_1^*(x^* - 1) \\ \nabla_1^* = 2(b-a) = \nabla_2 \\ \nabla_2^* = 2b+h \end{cases} \quad (37)$$

The set of Eq. (34) is singular. Therefore, its solution must be considered in the area of boundary layer problems. For the purpose of solving, MAM of the perturbation technique has been used. As boundary conditions are clamped-clamped, one lies in $x^* = 0$ and the other one in $x^* = 1$. So, the solution of the problem contains an outer solution away from the boundaries and two inner solutions near the two boundaries at $x^* = 0$ and $x^* = 1$ (Nayfeh 1993).

The problem solving is carried out in three areas: 1- Area away from the boundaries (Outer solution), 2- Boundary area $x^* = 0$ (inner solution at $x^* = 0$), 3- Boundary area $x = L$ (inner solution at $x^* = 1$). Final solution is obtained by combining the solutions above.

5. Results and discussion

The analytical solution described in the preceding section for a nonhomogeneous and isotropic clamped-clamped thick truncated conical shell with $a = 40$ mm, $b = 30$ mm, $h = 20$ mm and $L = 200$ mm will be considered for $n = +1$, $n = 0$ (Ghannad *et al.* 2009), and $n = -1$. The Young's Modulus in inner surface and Poisson's ratio, respectively, have values of $E_i = 200$ GPa and $\nu = 0.3$. The applied internal pressure is 80 MPa.

Fig. 2 shows the distribution of axial displacement at different layers. At points away from the boundaries, axial displacement does not show significant differences in different layers, while at points near the boundaries, the reverse holds true.

The distribution of radial displacement at different layers is plotted in Figs. 3. The radial displacement at points away from the boundaries depends on radius and length. According to Figs. 2 and 3, the change in axial and radial displacements in the lower boundary is greater than that of the upper boundary and the greatest axial and radial displacement occurs in the inner surface ($z = -h/2$).

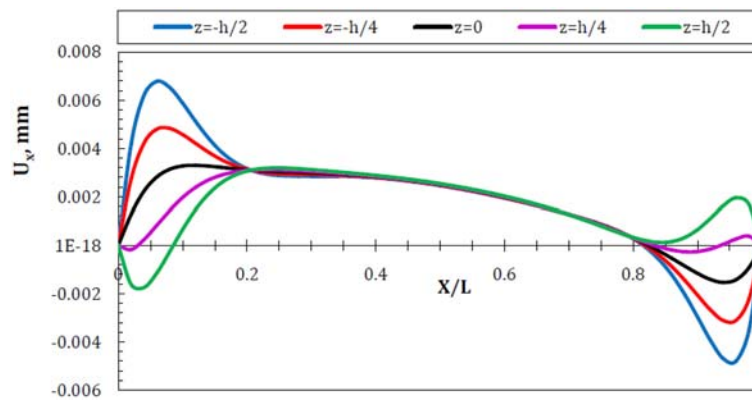


Fig. 2 Axial displacement distribution in different layers ($n = +1$)

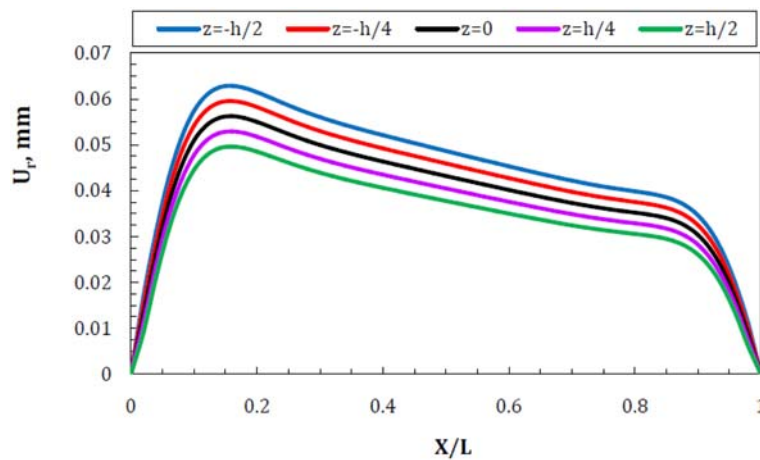


Fig. 3 Radial displacement distribution in different layers ($n = -1$)

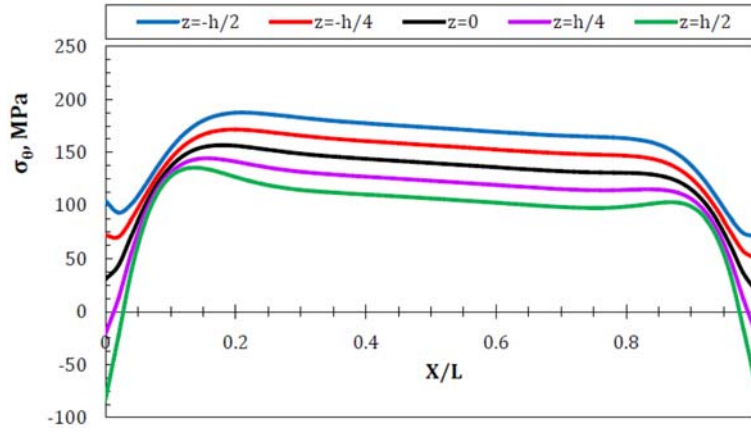


Fig. 4 Circumferential stress distribution in different layers ($n = +1$)

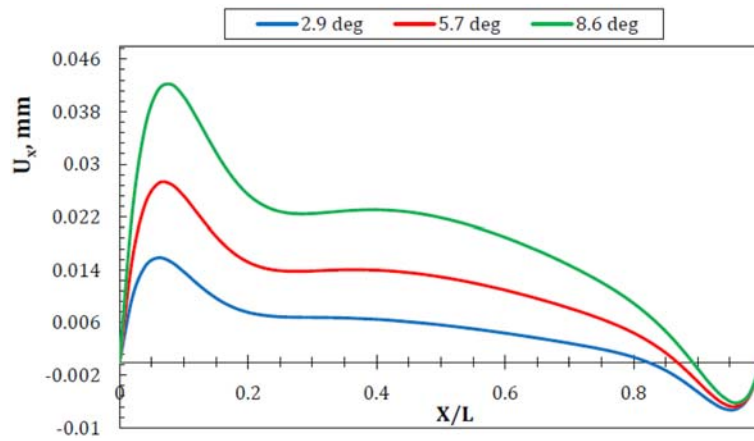


Fig. 5 Axial displacement distribution along inner surface with different tapering angles ($n = -1$)

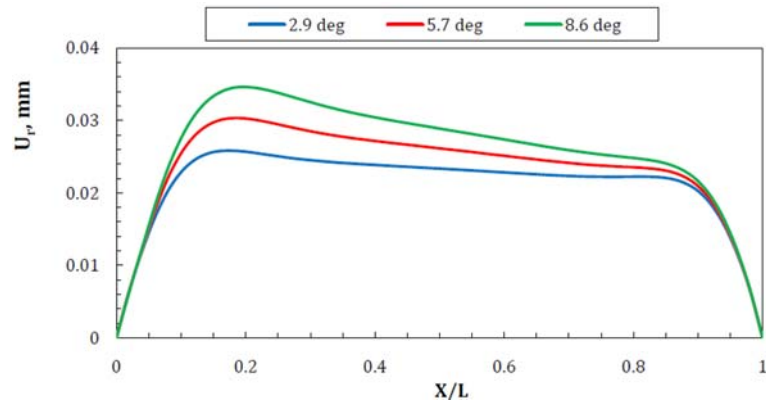


Fig. 6 Radial displacement distribution along inner surface with different tapering angles ($n = +1$)

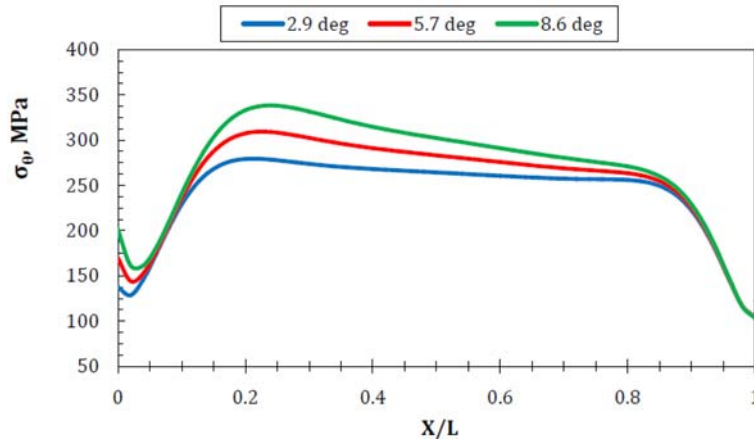


Fig. 7 Circumferential stress distribution along inner surface with different tapering angles ($n = -1$)

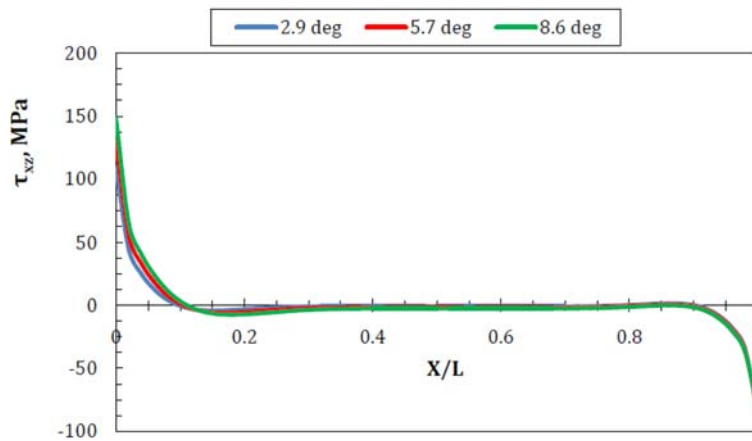


Fig. 8 Shear stress distribution along inner surface with different tapering angles ($n = +1$)

Distribution of circumferential stress in different layers is shown in Figs. 4 for $n = +1$. The circumferential stress at all points depends on radius and length. The greatest circumferential stress occurs in the inner surface ($z = -h/2$).

In Figs. 5 to 8, the effects of the changes in tapering angles on axial displacement, radial displacement, circumferential stress, and shear stress for $n = +1, -1$ will be considered. The distribution of axial displacement in the inner surface of the cone is shown in Fig. 5. The greater the tapering angle, the greater the displacement, which is significant. In cones with small tapering angles, the greatest axial displacement occurs in the lower boundary. The larger the tapering angles, the greater the axial displacement in the lower boundary and in the inner surface of the cone.

The distribution of radial displacement in the inner surface of the cone is shown in Fig. 6. The greater the tapering angle, the greater the radial displacement. The greatest radial displacement occurs in the lower boundary. In cones with small tapering angles, the greatest radial displacement occurs in the lower boundary. The larger the tapering angles, the greater the radial displacement in the lower boundary and in the middle surface of the cone.

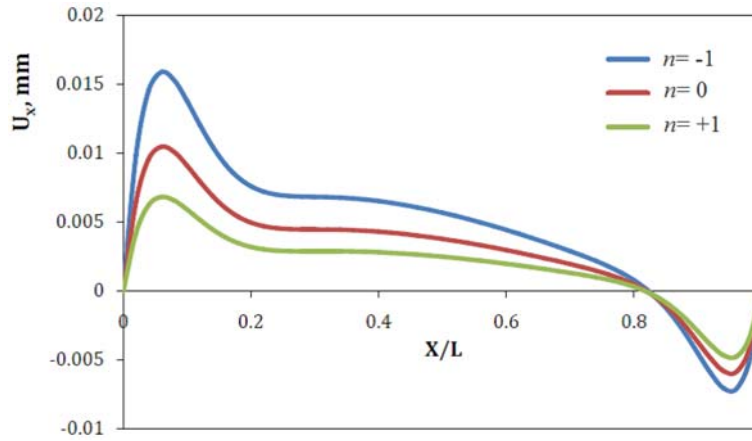


Fig. 9 Axial displacement distribution along inner surface ($n = -1,0,+1$)

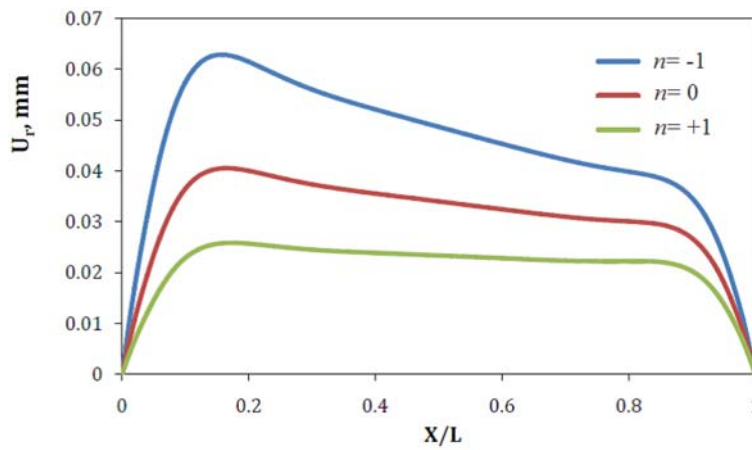


Fig. 10 Radial displacement distribution along inner surface ($n = -1,0,+1$)

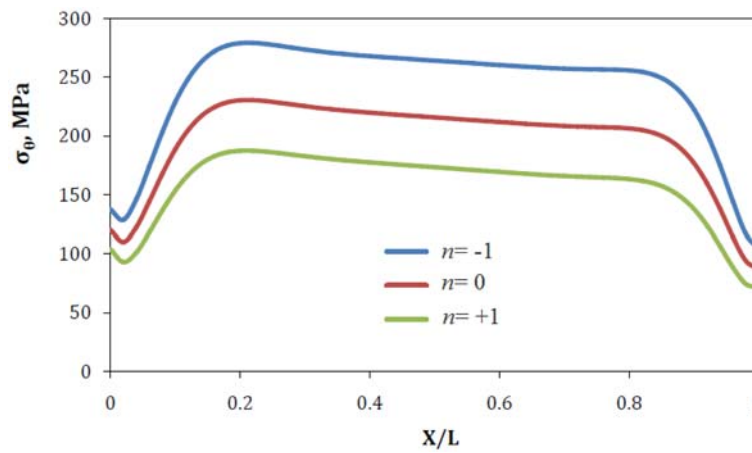


Fig. 11 Circumferential stress distribution along inner surface ($n = -1,0,+1$)

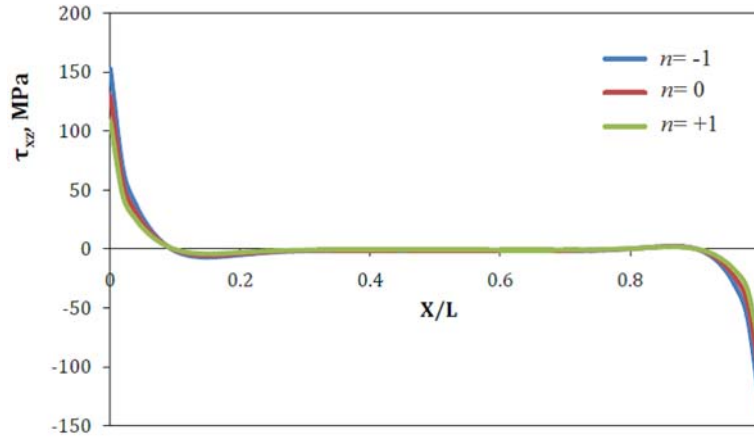


Fig. 12 Shear stress distribution along inner surface ($n = -1, 0, +1$)

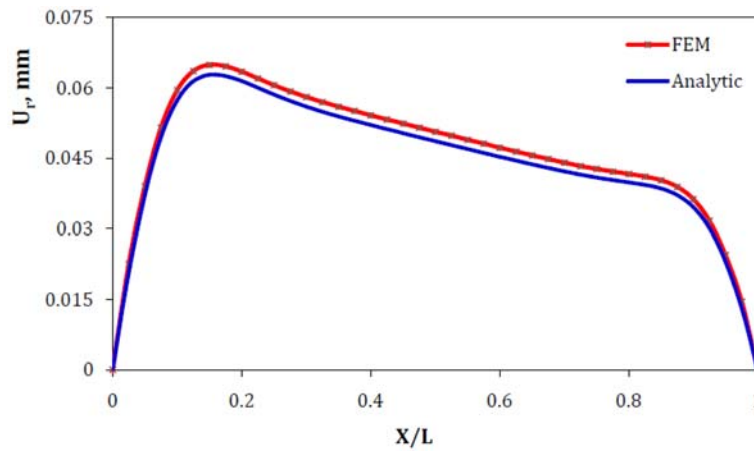


Fig. 13 Radial displacement distribution along inner surface ($n = -1$)

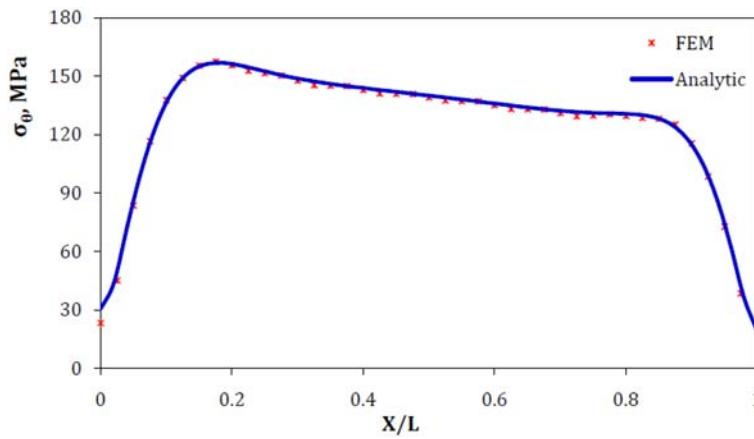


Fig. 14 Circumferential stress distribution along middle surface ($n = -1$)

In a similar manner, the distribution of the circumferential stress in the inner surface is illustrated in Fig. 7. As this figure suggests, the greater the tapering angle, the greater the circumferential stress.

The distribution of shear stress is shown in Fig. 8. According to this figure, the shear stress at points away from the boundaries is insignificant, and at boundary layers the changes in tapering angles do not have a significant bearing on the shear stress. The distribution of axial displacement for different values of n has been shown in Fig. 9. In the lower boundary, the difference between homogenous and nonhomogenous materials is significant. As the value of n increases, the axial displacement decreases.

The distribution of radial displacement for different values of n is shown in Fig. 10. The homogenous and nonhomogenous materials behave differently along the cone axis. In the lower boundary, the difference between the homogenous and nonhomogenous materials is significant. As the value of n increases, the radial displacement decreases.

The distribution of circumferential stress for different values of n is shown in Fig. 11. The homogenous and nonhomogenous materials behave differently along the cone axis. As the value of n increases, the circumferential stress decreases.

Fig. 12 shows the distribution of shear stress for different values of n . The shear stress at points away from the boundaries at different layers is the same and trivial. However, at points near the boundaries, the stress is significant.

Radial displacement and circumferential stress distributions are obtained using FSDT (analytical solution) are compared with the solutions of finite element method (FEM) and are presented in the form of graphs in the Figs. 13 and 14.

7. Conclusions

In the present study, making use of the FSDT, the analytical solution of thick isotropic FGM conical shells has been presented. The equilibrium equations, the energy principle and the FSDT, have been derived. The system of ordinary differential equations which are ordinary and have variable coefficients has been solved analytically, by using the MAM of the perturbation theory.

The axial displacement in thick conical shells at the boundaries depends on both length and radius whereas at points away from the boundaries, it depends on the length rather than the radius. The radial displacement at all points in a conical shell depends both on the radius and the length. The circumferential stress at different layers depends on the radius and the length. The greatest values of stress and displacement are observed in the inner surface. The shear stress at boundary layers is significant while at points away from the boundaries it is just the opposite. The axial displacement, radial displacement, and circumferential stress depend heavily on tapering angles and any change in the tapering angle leads to a change in them; while this is not the case for shear stress. As the value of nonhomogenous constant n increases, the axial displacement, the radial displacement and circumferential stress decrease. For the axial displacement, the homogenous and nonhomogenous materials behave the same and converge along the cone axis; whereas for the radial displacement and circumferential stress, these materials behave differently along the cone axis. The difference between homogenous and nonhomogenous materials is significant in the lower boundary for both the axial and radial displacements. In addition, for a comparative study, a geometry specimen was modeled using a commercial finite elements code, ANSYS 12 and good agreement was found between the analytical solutions (FSDT) and the solutions carried out through the FEM.

References

- Asemi, K., Akhlaghi, M., Salehi, M. and Zad, S.K.H. (2010), "Analysis of functionally graded thick truncated cone with finite length under hydrostatic internal pressure", *Arch. Appl. Mech.*, **81**, 1063-1074.
- Asemi, K., Salehi, M. and Akhlaghi, M. (2010), "Dynamic analysis of a functionally graded thick truncated cone with finite length", *Int. J. Mech. Mater. Des.*, **6**, 367-378.
- Asemi, K., Salehi, M. and Akhlaghi, M. (2011), "Elastic solution of a two-dimensional functionally graded thick truncated cone with finite length under hydrostatic combined loads", *Acta. Mech.*, **217**, 119-134.
- Chaudhry, H.R., Bukiet, B. and Davis, A.M. (1996), "Stresses and strains in the left ventricular wall approximated as a thick conical shell using large deformation theory", *J. Biol. Syst.*, **4**, 353-372.
- Eipakchi, H.R. (2010), "Third-order shear deformation theory for stress analysis of a thick conical shell under pressure", *J. Mech. Mater. Struct.*, **5**, 1-17.
- Eipakchi, H.R., Khadem, S.E. and Rahimi, G.H. (2008), "Axisymmetric stress analysis of a thick conical shell with varying thickness under nonuniform internal pressure", *J. Eng. Mech.*, **134**, 601-610.
- Eipakchi, H.R., Rahimi, G.H. and Khadem, S.E. (2003), "Closed form solution for displacements of thick cylinders with varying thickness subjected to nonuniform internal pressure", *Struct. Eng. Mech.*, **16**, 731-748.
- Ghannad, M., Nejad, M.Z. and Rahimi, G.H. (2009), "Elastic solution of axisymmetric thick truncated conical shells based on first-order shear deformation theory", *Mechanika*, **79**, 13-20.
- Ghannad, M. and Nejad, M.Z. (2010), "Elastic analysis of pressurized thick hollow cylindrical shells with clamped-clamped ends", *Mechanika*, **85**, 11-18.
- Ghannad, M., Rahimi, G.H. and Nejad, M.Z. (2012), "Determination of displacements and stresses in pressurized thick cylindrical shells with variable thickness using perturbation technique", *Mechanika*, **18**, 14-21.
- Hausenbauer, G.F. and Lee, G.C. (1966), "Stresses in thick-walled conical shells", *Nucl. Eng. Des.*, **3**, 394-401.
- McDonald, C.K. and Chang, C.H. (1973), "A second order solution of the nonlinear equations of conical shells", *Int. J. Nonlin. Mech.*, **8**, 49-58.
- Mirsky, I. and Hermann, G. (1958), "Axially motions of thick cylindrical shells", *J. Appl. Mech-T. ASME.*, **25**, 97-102.
- Naghdi, P.M. and Cooper, R.M. (1956), "Propagation of elastic waves in cylindrical shells, including the effects of transverse shear and rotary inertia", *J. Acoust. Soc. Am.*, **29**, 56-63.
- Nayfeh, A.H. (1993), *Introduction to Perturbation Techniques*, John Wiley, New York.
- Nejad, M.Z., Rahimi, G.H. and Ghannad, M. (2009), "Set of field equations for thick shell of revolution made of functionally graded materials in curvilinear coordinate system", *Mechanika*, **77**, 18-26.
- Ozturk, B. and Coskun, S.B. (2011), "The Homotopy Perturbation Method for free vibration analysis of beam on elastic foundation", *Struct. Eng. Mech.*, **37**, 415-425.
- Pan, D., Chen, G. and Lou, M. (2011), "A modified modal perturbation method for vibration characteristics of non-prismatic Timoshenko beams", *Struct. Eng. Mech.*, **40**, 689-703.
- Sundarasivaraoa, B.S.K. and Ganesan, N. (1991), "Deformation of varying thickness of conical shells subjected to axisymmetric loading with various end conditions", *Eng. Fract. Mech.*, **39**, 1003-1010.
- Takahashi, S., Suzuki, K. and Kosawada, T. (1986), "Vibrations of conical shells with variable thickness", *B. JSME.*, **29**, 4306-4311.
- Vlachoutsis, S. (1992), "Shear correction factors for plates and shells", *Int. J. Numer. Method. Eng.*, **33**, 1537-1552.

Appendix

Analytical solution for $n = -1$

In this case, the modulus of elasticity is as follows

$$E(x, z) = \frac{2E_i b L}{L(2a + 2z + h) - 2(a - b)x} \quad (\text{A1})$$

Forces and moments are obtained as follows

$$\begin{cases} N_x = \lambda E_i b \left[(1 - \nu) \frac{h}{R} \frac{du}{dx} + \nu \alpha \frac{w}{R} + \nu \left(\frac{2h}{R} - \alpha \right) \psi \right] \\ N_\theta = \lambda E_i b \left[\nu \alpha \frac{du}{dx} + \nu (h - R\alpha) \frac{d\phi}{dx} + (1 - \nu) \beta w + [\alpha - (1 - \nu) R\beta] \psi \right] \\ N_z = \lambda E_i b \left[\nu \frac{h}{R} \frac{du}{dx} + \nu \alpha \frac{w}{R} + \left(\frac{h}{R} - \nu \alpha \right) \psi \right] \end{cases} \quad (\text{A2})$$

$$\begin{cases} M_x = \lambda E_i b \left[(1 - \nu) \left(\frac{h^3}{12R} \right) \frac{d\phi}{dx} + \nu \left(\frac{h}{R} - \alpha \right) w + \nu (R\alpha - h) \psi \right] \\ M_\theta = \lambda E_i b \left[\nu (h - R\alpha) \frac{du}{dx} + \nu R (R\alpha - h) \frac{d\phi}{dx} + (1 - \nu) (\alpha - R\beta) w \right. \\ \left. + (h - R\alpha + (1 - \nu) R (R\beta - \alpha)) \psi \right] \\ M_z = \lambda E_i b \left[\nu \frac{h^3}{12R} \frac{d\phi}{dx} + \nu \left(\frac{h}{R} - \alpha \right) w + \nu (R\alpha - h) \psi \right] \end{cases} \quad (\text{A3})$$

$$Q_x = \frac{K}{2} (1 - 2\nu) \lambda E_i b \frac{h}{R} \left[\phi + \frac{dw}{dx} \right] \quad (\text{A4})$$

$$M_{xz} = \frac{K}{2} (1 - 2\nu) \lambda E_i b \frac{h^3}{12R} \frac{dw}{dx} \quad (\text{A5})$$

where

$$\begin{cases} \alpha = \ln \frac{(a + h)L - (a - b)x}{aL - (a - b)x} \\ \beta = \frac{L^2 h}{[(a + h)L - (a - b)x][aL - (a - b)x]} \end{cases} \quad (\text{A6})$$

Set of differential equations could be derived as follows

$$\begin{cases} \frac{d}{dx} \left([B_1] \frac{d}{dx} \{y\} \right) + \frac{d}{dx} ([B_2] \{y\}) + [B_3] \frac{d}{dx} \{y\} + [B_4] \{y\} = \{F'\} \\ \{y\} = \{u(x) \quad \phi(x) \quad w(x) \quad \psi(x)\}^T \end{cases} \quad (\text{A7})$$

where the coefficients matrices $[B_i]_{4 \times 4}$, and force vector $\{F'\}$ are as follows

$$[B_1] = \begin{bmatrix} (1-\nu)h & 0 & 0 & 0 \\ 0 & (1-\nu)\frac{h^3}{12} & 0 & 0 \\ 0 & 0 & \Lambda h & 0 \\ 0 & 0 & 0 & \Lambda\frac{h^3}{12} \end{bmatrix} \quad (A8)$$

$$[B_2] = \begin{bmatrix} 0 & 0 & \nu\alpha & \frac{\nu}{2L}(4hL - \alpha\Upsilon(x)) \\ 0 & 0 & \frac{\nu}{2L}(2hL - \alpha\Upsilon(x)) & \frac{\nu\Upsilon(x)}{4L^2}(\alpha\Upsilon(x) - 2hL) \\ 0 & \Lambda h & 0 & 0 \\ 0 & 0 & 0 & 0 \end{bmatrix} \quad (A9)$$

$$[B_3] = \begin{bmatrix} 0 & 0 & 0 & 0 & 0 & 0 \\ 0 & 0 & 0 & 0 & -\Lambda h & 0 \\ -\nu\alpha & -\frac{\nu}{2L}(2hL - \alpha\Upsilon(x)) & 0 & 0 & 0 & 0 \\ -\frac{\nu}{2L}(4hL - \alpha\Upsilon(x)) & -\frac{\nu\Upsilon(x)}{2L}\left(\frac{\alpha}{2L}\Upsilon(x) - h\right) & 0 & 0 & 0 & 0 \end{bmatrix} \quad (A10)$$

$$[B_4] = \begin{bmatrix} 0 & 0 & 0 & 0 \\ 0 & -\Lambda h & 0 & 0 \\ 0 & 0 & -(1-\nu)\beta & -\alpha + \frac{(1-\nu)\beta}{2L}\Upsilon(x) \\ 0 & 0 & -\alpha + \frac{(1-\nu)\beta}{2L}\Upsilon(x) & \frac{1}{L}(\alpha\Upsilon(x) - 2hL) - \frac{(1-\nu)\beta}{4L^2}(\Upsilon(x))^2 \end{bmatrix} \quad (A11)$$

$$\{F'\} = \frac{1}{\lambda E_i b} \left(a + \frac{\nabla_2}{2L} x \right) \begin{Bmatrix} -P_x \\ \frac{h}{2} P_x \\ -P_z \\ \frac{h}{2} P_z \end{Bmatrix} \quad (A12)$$

Taking du/dx as v , thus, set of differential equations could be derived as follows

$$\begin{cases} \frac{d}{dx} \left([A_1] \frac{d}{dx} \{y\} \right) + \frac{d}{dx} \left([A_2] \{y\} \right) + [A_3] \frac{d}{dx} \{y\} + [A_4] \{y\} = \{F\} \\ \{y\} = \{v(x) \quad \phi(x) \quad w(x) \quad \psi(x)\}^T \end{cases} \quad (A13)$$

where the coefficients matrices $[A_i]_{4 \times 4}$, and force vector $\{F\}$ are as follows

$$[A_1] = \begin{bmatrix} 0 & 0 & 0 & 0 \\ 0 & \frac{(1-\nu)h^3}{12} & 0 & 0 \\ 0 & 0 & \Lambda h & 0 \\ 0 & 0 & 0 & \Lambda \frac{h^3}{12} \end{bmatrix} \quad (\text{A14})$$

$$[A_2] = \begin{bmatrix} 0 & 0 & 0 & 0 \\ 0 & 0 & \frac{\nu}{2L}(2hL - \alpha\Upsilon(x)) & \frac{\nu}{4L^2}\Upsilon(x)(\alpha\Upsilon(x) - 2hL) \\ 0 & \Lambda h & 0 & 0 \\ 0 & 0 & 0 & 0 \end{bmatrix} \quad (\text{A15})$$

$$[A_3] = \begin{bmatrix} 0 & 0 & 0 & 0 \\ 0 & 0 & -\Lambda h & 0 \\ 0 & -\frac{\nu}{2L}(2hL - \alpha\Upsilon(x)) & 0 & 0 \\ 0 & -\frac{\nu}{4L^2}\Upsilon(x)(\alpha\Upsilon(x) - 2hL) & 0 & 0 \end{bmatrix} \quad (\text{A16})$$

$$[A_4] = \begin{bmatrix} (1-\nu)h & 0 & \nu\alpha & \frac{\nu}{2L}(4hL - \alpha\Upsilon(x)) \\ 0 & -\Lambda h & 0 & 0 \\ -\nu\alpha & 0 & -(1-\nu)\beta & -\alpha + \frac{(1-\nu)\beta}{2L}\Upsilon(x) \\ -\frac{\nu}{2L}(4hL - \alpha\Upsilon(x)) & 0 & -\alpha + \frac{(1-\nu)\beta}{2L}\Upsilon(x) & \frac{1}{L}(\alpha\Upsilon(x) - 2hL) - \frac{(1-\nu)\beta}{4L^2}(\Upsilon(x))^2 \end{bmatrix} \quad (\text{A17})$$

$$\{F\} = \frac{1}{\lambda E_i b} \left\{ \begin{array}{l} -\int P_x \left(a + \frac{\nabla_2}{2L} x \right) dx + C_0 \\ P_x \frac{h}{2} \left(a + \frac{\nabla_2}{2L} x \right) \\ -P_z \left(a + \frac{\nabla_2}{2L} x \right) \\ P_z \frac{h}{2} \left(a + \frac{\nabla_2}{2L} x \right) \end{array} \right\} \quad (\text{A18})$$